Journal of Engineering Physics and Thermophysics, Vol. 69, No. 5, 1996

SPECKLE TECHNIQUE FOR MEASUREMENT OF TURBULENCE CHARACTERISTICS

N. A. Fomin and D. É. Vitkin

UDC 533.12.08+535.31:536.24

The possibilities of speckle photography for determination of the characteristics of turbulence for gas-dynamic flows are analyzed. It is shown that by using two-exposure speckle photography, the energy spectrum and the scales of turbulence can be calculated, while one-exposure speckle photography provides information on the energy and anisotropy of turbulent pulsations.

Introduction. A major class of optical methods of investigating turbulent flows is based on the direct linear dependence of the refractive index of a medium on its density

$$n - 1 = K\rho . \tag{1}$$

The pulsations of density in turbulent subsonic flow are usually small. However, in connection with the fact that the characteristic dimensions of density heterogeneities are also small, the density gradients turn out to be large, and turbulence manifests itself clearly on shadow and schlieren photographs of the flow [1].

In the case of isotropic turbulence, density pulsations in a turbulent flow can be described using a three-dimensional scalar random field; for anistropic turbulence, this field will be a vector one.

In the general case, the relationship between a three-dimensional pulsating field and a plane wave front of probing radiation that is produced by it is very complicated and often ambiguous. In a number of cases, for anisotropic turbulence relationships between the energy spectrum of density pulsations and the spectrum of two-dimensional thermal patterns that register distortion of the wave front in the near zone have been obtained [2-4].

Despite the difficulties of a quantitative processing of direct-shadow and schlieren photographs, the approach proposed in these works has been extended to investigations of turbulent flows [5-7]. At the same time, in recent years the possibility of very accurate quantitative measurement of the distortion of a plane wave front using speckle photography has been demonstrated. These measurements are performed using specialized automated systems for processing specklograms and make it possible to obtain quantitative information on the distortion of the wave front at tens and hundreds of thousands of points [8]. This opens up fresh opportunities for measuring the characteristics of turbulence using this technique.

2. Two-Exposure Speckle Photography. Unlike shadow photography, two-exposure speckle photography records the field of the angles of deviation for light beams that pass through the flow in question, i.e., $\varepsilon_x(x, y)$ and $\varepsilon_y(x, y)$ (see Fig. 1a). Based on these data, in [9-11] two-point correlation functions of the angles of deviation $R_{\varepsilon\perp}$ and $R_{\varepsilon\parallel}$ were calculated, from which the correlation functions of the turbulent pulsations were subsequently determined:

$$R_{\varepsilon_\perp}(\tau) = \frac{1}{m_p - \tau + 1} \sum_{j=0}^{m_p - \tau} \varepsilon_q(j, q)\, \varepsilon_q(j + \tau, q) ,$$

$$R_{\varepsilon\parallel}(\tau) = \frac{1}{n_q - \tau + 1} \sum_{i=0}^{n_q - \tau} \varepsilon_q(p, i)\, \varepsilon_q(p, i + \tau) . \tag{2}$$

Academic Sientific Complex "A. V. Luikov Heat and Mass Transfer Institute, Academy of Sciences of Belarus," Minsk, Belarus. Translated from Inzhenerno-Fizicheskii Zhurnal, Vol. 69, No. 5, pp. 805-810, September-October, 1996. Original article submitted July 17, 1994.

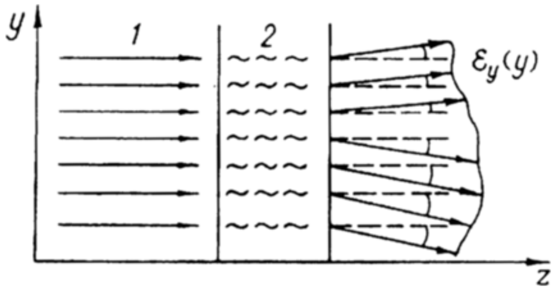

Fig. 1. Illustration of the deformation of a wave front (1) when it passes through a turbulent medium (2).

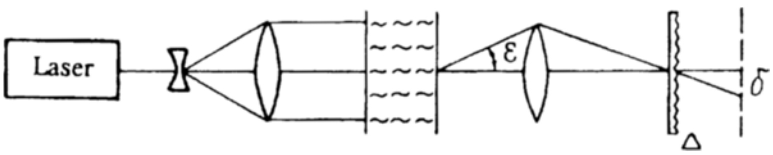

Fig. 2. Diagram of a pilot unit.

With allowance for the fact that the angles of deviation for light beams are determined by the integrals along the optical path of the corresponding density gradients (see, for example, [8]), we obtain

$$R_\varepsilon(\eta, \zeta) = -K_{GD}^2 \int_0^L \int_0^L \frac{\partial^2}{\partial \zeta^2} (R_\rho(\xi, \eta, \zeta))\, dx' dx'' . \quad (3)$$

when $L \to \infty$, i.e., L is much larger than the existing scale of turbulence, and for the case of isotropic turbulence from (3) we obtain an integral relation for the correlation functions of the density and the angles of deviation:

$$R_\rho(r) = \frac{1}{2K_{GD}^2 L\pi} \int_\tau^\infty \frac{1}{\sqrt{r^2 - \tau^2}} R_{\varepsilon_\perp}(\tau)\, d\tau . \quad (4)$$

Using the correlation density functions, we calculate different scales of turbulence, including its macro- and microscales:

$$L_\rho = \int_0^\infty \frac{R_\rho(r)}{R_\rho(0)}\, dr, \quad \lambda_\rho^2 = -2\frac{R_\rho(0)}{R_\rho''(0)} . \quad (5)$$

3. Description of the Experimental Procedure. The optical train of the pilot unit is presented in Fig. 1b. When investigating fast processes a Q-switched ruby laser ($\lambda \approx 0.69\ \mu$m, $E \approx 50$ mJ, and $\tau \approx 50$ nsec) served as a brightening source. The radiation was collimated by a system of the lenses L_1 and L_2 and the formed plane-parallel electromagnetic wave was guided to the phase object in question. The image of the distorted wave front from a plane at a distance Δ_2 from the phase object was projected on a matte plate, which was the generator of the speckle field and simultaneously the screen for observing the direct-shadow pattern of the flow, with the sensitivity of the optical train determined by the distance Δ_2.

The speckle field was photographed on the photoplate twice: once without the phase object (reference exposure) and then in its presence. In this case, due to refraction in the turbulent field of the flow, there was displacement of the speckles at each point of the specklogram by the value

$$\delta(x, y) = \varepsilon(x, y)\, \Delta_2 m_4 . \quad (6)$$

To determine the displacements field, we must measure the speckle displacement in speckle pairs of the corresponding sections of the specklogram. These displacements are calculated by the Young interference fringes

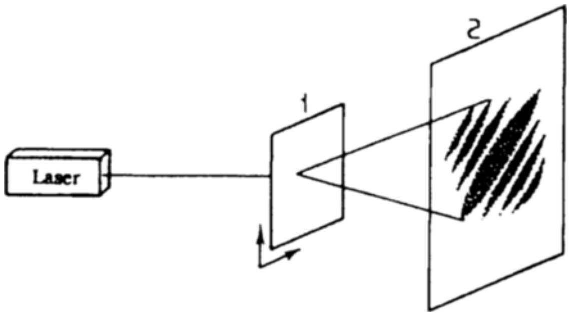

Fig. 3. Scheme of an automated system of specklogram processing: 1) specklogram on scanner, 2) Young fringes on a screen.

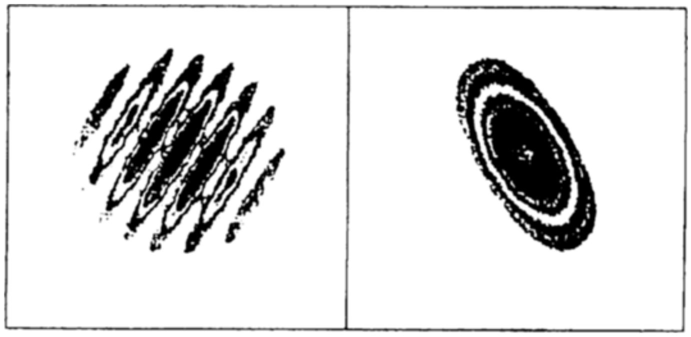

Fig. 4. Examples of the Young interference fringes.

that occur behind the specklogram in pointwise transillumination by a thin laser beam, for which it is necessary and sufficient to measure the distance between the maxima and the minima of the fringes and their slope to one of the axes. In this case, information can be read in the smallest steps provided by the scanning system. The number of readouts obtained on one specklogram is large; so, in processing of a specklogram on a 9 × 12 cm photoplate with a scanning step of 0.5 mm, for each coordinate we obtain about 25,000 number pairs. Processing of these and even substantially smaller amounts of experimental data calls for the creation of automated systems of data acquisition and processing. A diagram of an automated system for processing of two-exposure speckle photographs by interference fringes that, in this case, have the form of straight equidistant bands is shown in Fig. 3. The measuring system incorporates, in addition to a personal computer, an image input device (a video camera with an interface) and a scanner. The system makes it possible with high accuracy and spatial density to measure the local displacement of the speckle field formed on specklograms in experiments using the speckle technique.

We describe the main component parts of the measuring system.

Scanner. It is a two-coordinate program-controlled device connected to the printer port of the personal computer with a scanning step of 100 μm and higher. The device can operate both in the programmable mode and in the mode of manual control.

Image-Input Board. The interface is a board designed for inputting TV images into a IBM PC computer. A standard TV signal is fed from a TV camera to the board input. An output to a TV monitor is provided.

Connectors for the TV camera and the monitor are brought to the rear remote panel.

The circuit of the board consists of analog and digital parts. The analog part corrects the TV signal, amplifies it, and carries out its analog-to-digital conversion. Thereafter, the digital signal is converted to an analog one for the control monitor. The digital part of the circuit stores the code in the buffer memory of the board (the memory capacity is 64 kbyte of 6-bit words). The board has an IBM PC bus interface, and the computer can read data stored in the memory. Furthermore, the digital part of the board synchronizes the operation of the analog circuits. Using the board to introduce a standard TV signal into the IBM PC AT, we can input any standard TV signal from a TV camera based on a vidicon or a CCD array, from a TV set, from a scanning microscope, or any other device at the output of which a standard TV signal is produced.

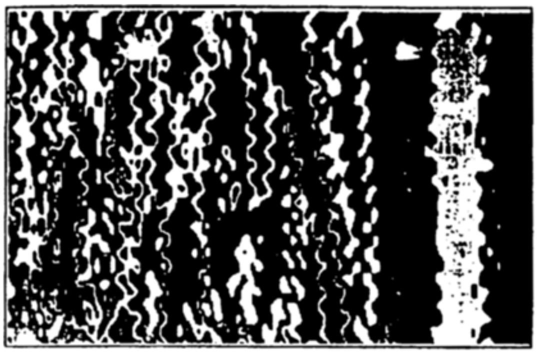

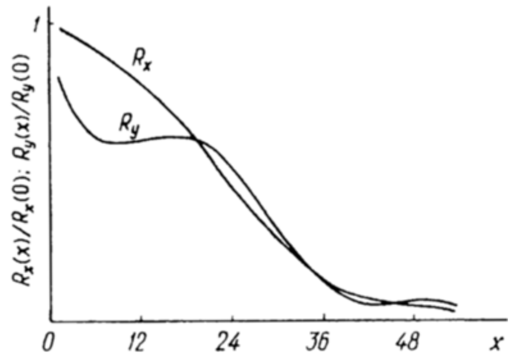

Fig. 5. Isolines of the angles of light deviation obtained experimentally.

Fig. 6. Calculated correlation functions of density in turbulent flow for one of the shears of a flow. x, mm.

The errors in determining theparameters for a contrast of the interference fringes of 100% are 0.3% for the slope and 0.6% for the period of the fringes. Processing of one image, depending on the algorithm parameters chosen by the user and the configuration of the personal computer (in our case, AT 386/387), can take 0.5 to 5 sec.

Figure 5 shows an example of a field of angles of deviation for light beams in turbulent flow that has been reconstructed from a specklogram. The flow field of propane flowing out of four nearby cylindrical holes was investigated as an example of flow with isotropic turbulence. The diameter of the illuminated part of the jet was equal to 8 cm; the distance from the matte plate to the focal plane (Δ_2) was 4 mm; the image (m_4) was 1:1. The number of points in this field was 64 × 64 = 4096. It took several hours to process the specklogram. Figure 6 gives an example of the correlation functions of density in turbulent flow for one of the flow sections obtained from these data. The micro- and macroscales of turbulence calculated by these functions were 2.4 mm and 25.2 mm.

4. One-Exposure Technique. In two-exposure speckle photography, the duration of each exposure should be much smaller than the time in which the speckles shift by distances comparable with their dimensions. In [12] it was noted that for a pulse duration that corresponds to appreciable displacements of speckles in the time between exposures, the diffraction halo becomes elliptical. In that work, a displacement by one speckle diameter

$$\Delta\tau \leq \frac{\sigma}{v_{\max} m}. \tag{7}$$

was considered acceptable.

More recently, in [13], it was proposed to use the ellipticity of a different halo to determine the speckle displacement during an exposure. In particular, the possibility of using this measurement to determine the velocity of motion for a rough surface (by the example of disk rotation) by a one-exposure speckle photograph of a moving surface with an extended exposure time was dealt with. As applied to the investigation of turbulent flows, one-exposure speckle photography was used in [9-11].

One-exposure speckle photography can be realized with any of the optical systems for the two-exposure technique described in [8]. In particular, use can also be made of a system with simultaneous production of a shadowgraph of the flow, which is presented in Fig. 2.

As far as data reduction is concerned, an optical device made employing this system can be represented as a system that consists of three main links:

1) $\langle \varepsilon^2 \rangle = k_1 \langle n'^2 \rangle$ – the average angle of light deviation is proportional to the average deviation of the refractive index;

2) $\Delta_i = k_2 \langle \varepsilon_i^2 \rangle^{1/2}$ – the light deviation on the matte plate corresponds to the angle of deviation;

3) the ratio of the axis lengths for the ellipse of speckle spreading on the photoplate enables us to judge the degree of anisotropy of the medium at a given point, and its position relative to the coordinate axes makes it possible to judge the direction of propagation of the flow anisotropy.

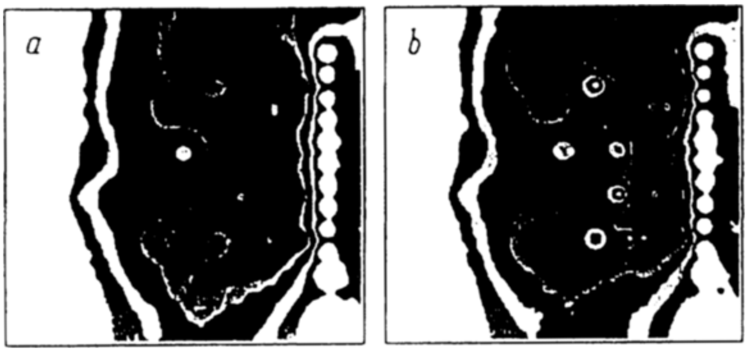

Fig. 7. Two-dimensional fields of turbulence calculated from experimental data.

In transillumination of a processed photoplate that contains similar ellipses by a thin laser beam an interference fringe of elliptical structure develops on a screen behind the photoplate. This ellipse is perpendicular to the ellipses on the photoplate and the ratio of the axis dimensions in them is similar.

We consider what information can be obtained from the described experiment.

Fluctuations of the angle of propagation of light beams that pass through an investigated volume of a turbulent medium carry information on the properties of the turbulence itself. An important characteristic of turbulence can be [14] the structure function, which is determined for pulsations of the refractive index of the medium as [15]

$$D_0(r) = \langle n'^2 \rangle = \langle (n_1 - n_2)^2 \rangle = C_0^2 r^{2/3} . \tag{8}$$

Here C_0^2 is the structure constant of the medium; r is the distance between two points with local values of the refractive index n_1 and n_2.

Relation (8) holds for the inertial region of turbulence, i.e., when the condition $l << r << L_0$ is satisfied. Here L_0 is the external scale of turbulence; l is the internal scale of turbulence, which is comparable with the correlation radius of optical inhomogeneities.

The structure function $\langle n'^2 \rangle$ characterizes the intensity of refractive index pulsations in a medium with scales that do not exceed r in the order of magnitude.

We can relate the structure function of the field of the refractive index for a medium to the fluctuations of the angle of the deviation of light beams. When the distance L traveled by a light wave in a turbulent medium satisfies the condition $L << l^2/\lambda$, where λ is the light wavelength, we can use an approximation of geometrical optics. According to [16], for an isotropic medium, the relation

$$\langle \varepsilon^2 \rangle = 2/3 \langle n'^2 \rangle L/l . \tag{9}$$

holds true. Here $\langle \varepsilon^2 \rangle$ is the variance of the angle of light deviation at the exit from the volume in question.

From relation (9) it is clear that, by measuring the fluctuation of the arrival angle of light beams, we can determine an important characteristic of turbulence, i.e., the structure function or the structure constant of the medium.

In a speckle-photography experiment we can determine not only the variance of the angle of light deviation (the speckle spreading $\sigma_1 = 1.22\lambda L_1/R_1 - \sigma$, where σ is the value of the speckle on the specklogram for the speckle field in the same train when the flow in question is absent, R_1 is the radius of the diffraction halo in processing of a specklogram with recorded disturbances of the medium) but also the flow anisotropy at each point

$$\frac{\langle \varepsilon_x^2 \rangle^{1/2}}{\langle \varepsilon_y^2 \rangle^{1/2}} = \frac{\Delta_x}{\Delta_y} . \tag{10}$$

The flame of a propane-butane burner was chosen as an object the anisotropy in which was investigated using speckle technology. The turbulent region of the flame was photographed by one-exposure speckle photography using an LG-38 helium-neon laser. The exposure time was 10 sec for a VRL high-resolution (1000 lines/mm) photoplate with a laser power of 30 mW. The size of the transilluminated region was approximately 40 × 60 mm. Figure 7a shows a field of values of flow anisotropy calculated by the ellipses of spreading and Fig. 7b gives the field of the intensity of turbulent pulsations along one of the coordinates (d_0/d_m).

Therefore, the work has demonstrated the possibilities of a new experimental technique, i.e., speckle photography, for investigating turbulent flows. In particular, it is shown that one-exposure technology is a simple and convenient method for quantitative determination of the absolute value of turbulence anisotropy simultaneously over the entire field of the flow; the optical system does not require calibration by other methods.

The authors express their thanks to the International Scientific Foundation for the support of this work (Grant RWB000).

NOTATIONS

n, refractive index; ρ, density; K, Gladstone–Dale constant; x, y, η, ξ, coordinates; ε, angle of light deviation; $R_{\varepsilon\parallel}$ and $R_{\varepsilon_\perp}$, correlation functions; p, q, i, j, m, n, whole numbers (indexes); L_ρ, λ_ρ, macro- and microscales of turbulence; Δ_2, distance from the generator of the speckle field to the focal plane; s, width of the Young interference fringes; m, magnification of the optical train; σ, value of the speckle on the specklogram in photography of speckle field in the absence of the flow in question; L_1, distance from the specklogram to the screen in the reproduction circuit; d_0, halo diameter in diffraction of laser beam by undisturbed speckle field; d_m, dimension of the minor axis of the ellipse.

REFERENCES

1. R. U. Ladenburg (ed.), Physical Measurements in Gas Dynamics [in Russian], Moscow (1957).
2. F. J. Weyl, Nav. Ord. Rept., 211-245 (1945).
3. L. S. G. Kovasznay, Heat Transfer and Fluid Mechanics Institute, Berkeley, Calif. (1949), Publ. by Am. Soc. Mech. Engns.(1949).
4. M. S. Uberoi and L. S. G. Kovasznay, Project Squid. Tech. Rept., **30** (1951).
5. M. S. Uberoi and L. S. G. Kovasznay, Quart. Appl. Math., **10**, 375-393 (1953).
6. M. S. Uberoi and L. S. G. Kovasznay, J. Appl. Phys., **26**, 19-24 (1955).
7. L. S. Taylor, Analysis of Turbulence by Shadowgraph, AIAA J., **8**, 1284-1287 (1969).
8. N. A. Fomin, Speckle Interferometry of Gas Flows [in Russian], Minsk (1989).
9. R. Erbeck and W. Merzkirch, Experiments in Fluids, **6**, 89-93 (1988).
10. J. Keller, Statistische Turbulenzanalyse isotroper dichtefelder unter Anvendung der Specklephotography: Verstarkung mit einem Senkrechten Verdchtungsstoss, Dissertation, Universität Essen (1989).
11. K. Oberste–Lehn, Speckle-photographische Untersuchungen eines turbulenten passiven Skalarfeldes bei hohen Amplituden der Temperaturfluktuationen, Dissertation, Universität Essen (1991).
12. L. Lourenco, Von Karman Institute for Fluid Dynamics Lecture Series 1986-09, 1-63 (1986).
13. C. S. Narayanamurthy, Appl. Opt., **39**, No. 22, 3157-3199 (1991).
14. A. N. Kolmogorov, Dokl. Akad. Nauk SSSR, **30**, No. 4, 301-305 (1941).
15. A. M. Obukhov, Izv. Akad. Nauk SSSR, Fiz. Atm. Okeana, **8**, No. 1 (1968).
16. M. M. Weiner, Appl. Opt., **6**, No. 11 (1967).